Burns & Trauma, 2020, 8, tkaa013
doi: 10.1093/burnst/tkaa013
Technical Report

Technical Report

A modified scar model with controlled tension on secondary wound healing in mice

Zi Wang#, Xin Huang#, Tao Zan, Qingfeng Li* and Haizhou Li*

Department of Plastic and Reconstructive Surgery, Ninth People's Hospital, Medical School of Shanghai Jiao Tong University, 639 Zhizaoju Road, Shanghai 200011, China

*Correspondence. Qingfeng Li, Email: dr.liqingfeng@shsmu.edu.cn; Haizhou Li, Email: daniel.Lihaizhou@icloud.com

#These authors contributed equally to the work

Received 3 December 2019; Revised 19 December 2019; Editorial decision 2 March 2020

Abstract

Pathological scars might cause a distorted appearance and restricted mobility, and the study of scar pathophysiology has been hindered by the absence of a reliable model. In this study, we introduce a model with a modified device to induce controlled tension on a wound healing by secondary intention to overcome the shortcomings of the model generated by Aarabi *et al*. We investigated and recommend an induction of 0.1 N/mm^2 tension on day 7 for 14 days to mimic the characteristics of human scars. A 3.5-fold increase in scar tissue and a 2-fold increase in collagen production were induced by the modified model. Histologically, the modified method increased scar thickness. However, no significant difference was found in cell density between the two groups. This modified procedure significantly increased scar tissue, which could be used for further cellular and biomolecular research. The mechanical force applied to the wound became measurable and controllable. This method is more convenient for researchers to observe in real-time and for providing timely adjustments of the tension used in this modified model.

Key words: Scar model, Mechanical force, Murine model, Wound healing

Background

Pathological scar formation is a common complication following trauma, surgical incision and burn injuries (1) that often leads to distortion and restricted mobility (2). Since its pathophysiology remains poorly understood, none of the main treatments can completely prevent scar formation; the patient outcomes have shown significant differences among individuals (3, 4). Compared to similar diseases, targeted therapies for scar progressed slowly (5, 6). A major reason may be the current lack of a proper *in vivo* model to simulate the formation of human scars to test potential new treatments (7).

Various animal models mimicking the wound healing of humans have been established over the past half-century (8–10). However, the skin structures of humans and animals are different. As reported, the resting tension of murine skin is lower than that of normal human skin (11–13). Thus, the application of these models may lead to misunderstandings about the wound repair process of the human body. To solve this problem, Aarabi *et al*. first reported that a murine model with a healing wound on the dorsum produced pathological scars when additional mechanical force was applied (14). Since the same procedure could be conducted on gene knockout mice, this model may contribute to a more in-depth understanding of the pathophysiological mechanisms of scar formation.

However, the first reported method (15) induced few scar tissues for further study. The method to create mechanical force was difficult for researchers to operate, and thereby

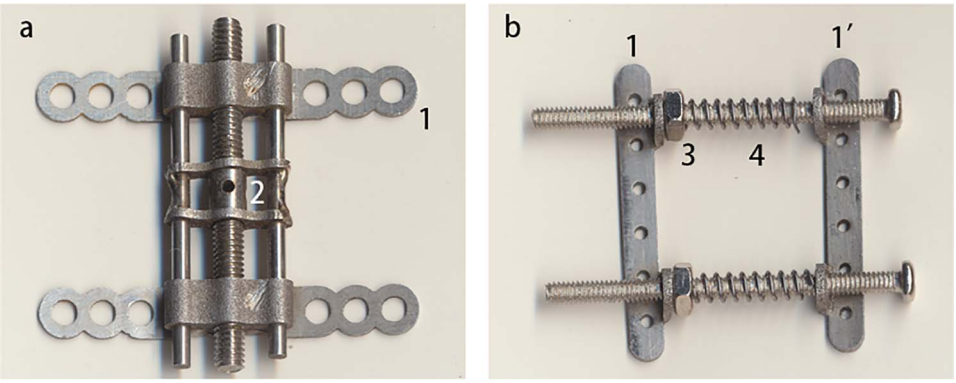

Figure 1. Previously reported and modified devices for the scar model. **(a)** previous stretching device: an expansion screw (2) was rotated to stretch two stainless steel plates (1). **(b)** Modified stretching device: a fixed plate (1) and a movable plate (1′) were to be sutured at both sides of the healing wound. The movement of the nut (3) compressed the spring (4) and pushed the movable plate (1′) to apply skin tension, which was visualized as the total compression of the spring

obtain reproducible results. The measurement of the applied force was done after murine skin specimens were obtained, and mouse skin was analysed *ex vivo* to determine the amount of force required to create a level of stress equivalent to that experienced by human skin *in vivo*. As a result, the applied force was uncontrollable in real-time and caused significant individual differences in the induced scars.

To overcome the above limitations, we modified the previously reported scar model with controlled tension to normalize the force applied to each animal and changed the healing wound from a primary closed wound to a secondary wound to obtain more tissue identical to human scars. We assessed the model by examining the histopathological characteristics of scars induced by this method.

Methods

Animals

Animal procedures were all approved by the Committee on the Ethics of Animal Experiments of Shanghai Jiao Tong University School of Medicine. Male C57BL/6 mice of specific pathogen-free grade, 6 weeks old and weighing 25 ± 3 g were purchased from the Shanghai Experimental Animal Center. All procedures were completed under strict aseptic manipulation. Mice were sacrificed at designated time points, and scar tissue was fixed in 10% formalin for histological staining or incubated overnight at 4°C in an acid-pepsin extraction for soluble collagen assay.

Previous procedure

The previous scar model from Aarabi *et al.* was to create a 2-cm, linear full-thickness incision on the dorsum of the mouse, then reapproximate the wound with 6–0 nylon sutures. The sutures were removed on day 4 post-incision. Subsequently, the incisional scar was challenged with stretching force via a skin-stretching device (Fig. 1a). According to the description of the authors (10), the expansion screws need to be stretched by 2 mm on day 4 post-incision and by 4 mm every other day thereafter to maintain the force from the natural elongation of skin.

Modified procedure

In our study, the linear incision was modified to a 2×0.5 cm full-thickness wound on the dorsum of the mouse, and a silicone splint was applied around the wound. The splint was fixed with cyanoacrylate adhesives and consolidated with 6–0 nylon sutures. After granulation tissue filled the wound in 7 days with minimal contracture, the wound was ready for additional skin tension. On day 7 post-incision, the silicone splint was removed and two stainless steel plates were fixed to both sides of the granulation tissue (Fig. 2). There were two different plates, one fixed with the screw and the other removable (Fig. 1b). The nut was adjusted to be away from the fixed plate and compress the spring, with the removable plate forming a controllable mechanical force on the skin. The tension was estimable and manageable by adjusting the nut. In total, the tension was applied to the skin for 14 days.

To determine the time of loading, one group of mice per day were sacrificed to study the histological changes. To decide the accurate mechanical force used to induce additional scar formation, mice were sacrificed to observe changes of scars with different tensions after 14 days.

Biomechanical analysis

On day 7, after granulation tissue mostly filled the wound, the induced scar was removed from animals and was measured to study the thickness and width of granulation. Since we made a 2×0.5 cm full-thickness wound, the length of the granulation was known. Based on the first batch of mice that were executed, we were able to discern an average value of the thickness of granulation. The tension (cross-sectional area tension = [length of spring compression $\times$ the elastic coefficient of the spring $\times$ 2]/[thickness of granulation $\times$ length of granulation]) applied to murine wounds by our device was readable by researchers in real-time.

Histology

On designated days after wound stretching, the induced scar was removed from animals.

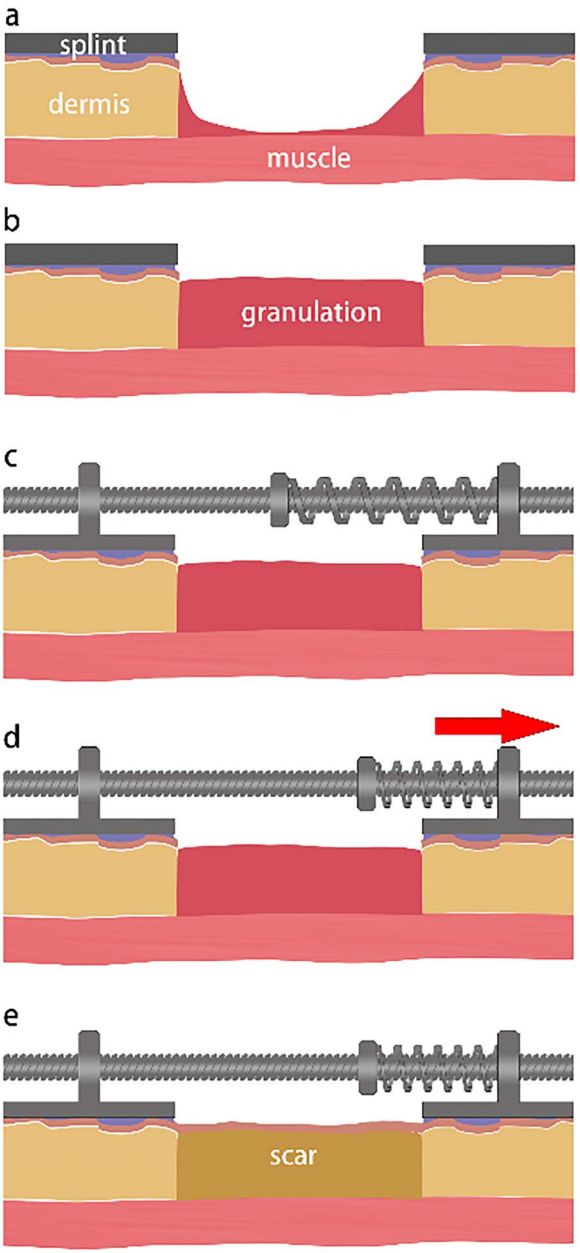

Figure 2. Illustration of the modified scar model. **(a)** A 2 × 0.5 cm full-thickness wound was created with scissors and the surrounding skin was fixed with a splint. **(b)** Granulation filled the wound within 7 days. **(c)** The stretching device was fixed to the surrounding skin with 3–0 silk thread sutures immediately after the remove of the splint. **(d)** The nut was adjusted to compress the spring and thus push the movable plates away. **(e)** The mechanical force was maintained for 14 days until the re-epithelialization of the granulation and scar remodeling

Samples of human hypertrophic scars were harvested from Shanghai Ninth People's Hospital. All procedures were followed and ethical approval from the Human Research Ethics Committee of Shanghai Jiao Tong University School of Medicine was obtained. Sections (5 μm thick) were prepared, using hematoxylin and eosin and picrosirius red staining to assess the produced collagen. Differences in the histological architecture and scar thickness, as well as the width of the scars induced by the modified and previous procedure induced scars were assessed using an upright microscope (Nikon ECLIPSE Ni, Japan) with polarizer accessories. Nuclear staining with 6-diamidino-2-phenylindole was performed. Data were expressed as cell counts and cellular density per 0.1 mm^2.

Images were collected and then evaluated blindly by two independent researchers using ImageJ (NIH Image, USA) image analysis software, and no difference was found in their data. The results are presented as the mean ± standard deviation (SD).

Sircol^{TM} Soluble Collagen Assay

The Sircol^{TM} Soluble Collagen Assay Kit (Biocolor, Carrickfergus, UK) was used to determine the total collagen content of scars. Manufacturer's instructions were strictly followed in all procedures. Data were expressed as the collagen content of the entire scar.

Statistical analysis

Each treatment group consisted of 6 mice. GraphPad Prism 7 (GraphPad Software, La Jolla, CA 92037 USA) was used to analyse the data. Comparisons were made using two-tailed Student's unpaired *t*-test. Values are presented as the mean ± SD. Significance was set at $p < 0.05$.

Results

Time of loading and tension to induce scar

To induce scars on a secondary healing wound, wound dehiscence after the load of mechanical force should be avoided. We established a 2 × 0.5 cm full-thickness wound fixed with a splint and studied the histological changes of granulation thickness and epithelial gap over time (Fig. 3). We found the granulation mostly filled the wound in 7 days with minimal wound contraction.

To determine the precise mechanical force used to induce additional scar formation, we observed changes in the collagen content of the scars with different tensions for 14 days. Scars induced with 0.05 N/mm^2, 0.1 N/mm^2 and 0.2 N/mm^2 of tension produced significantly higher collagen. Then, we tested if the murine skin was sustainable under such tension. During the entire procedure, devices were checked every 12 hours and refixed if they became detached from the skin. A total of 0.2 N/mm^2 skin tension caused unstable results because of the injuries induced by high-tension sutures.

Modified model showed more obvious histopathological characteristics of scar

We modified the scar model from that reported by Aarabi *et al.* The linear incision was changed to a 2 × 0.5 cm full-thickness wound to obtain more scar tissue, and the mechanical force was loaded for 14 days in both the previous and modified methods (Fig. 4). The mice were sacrificed for

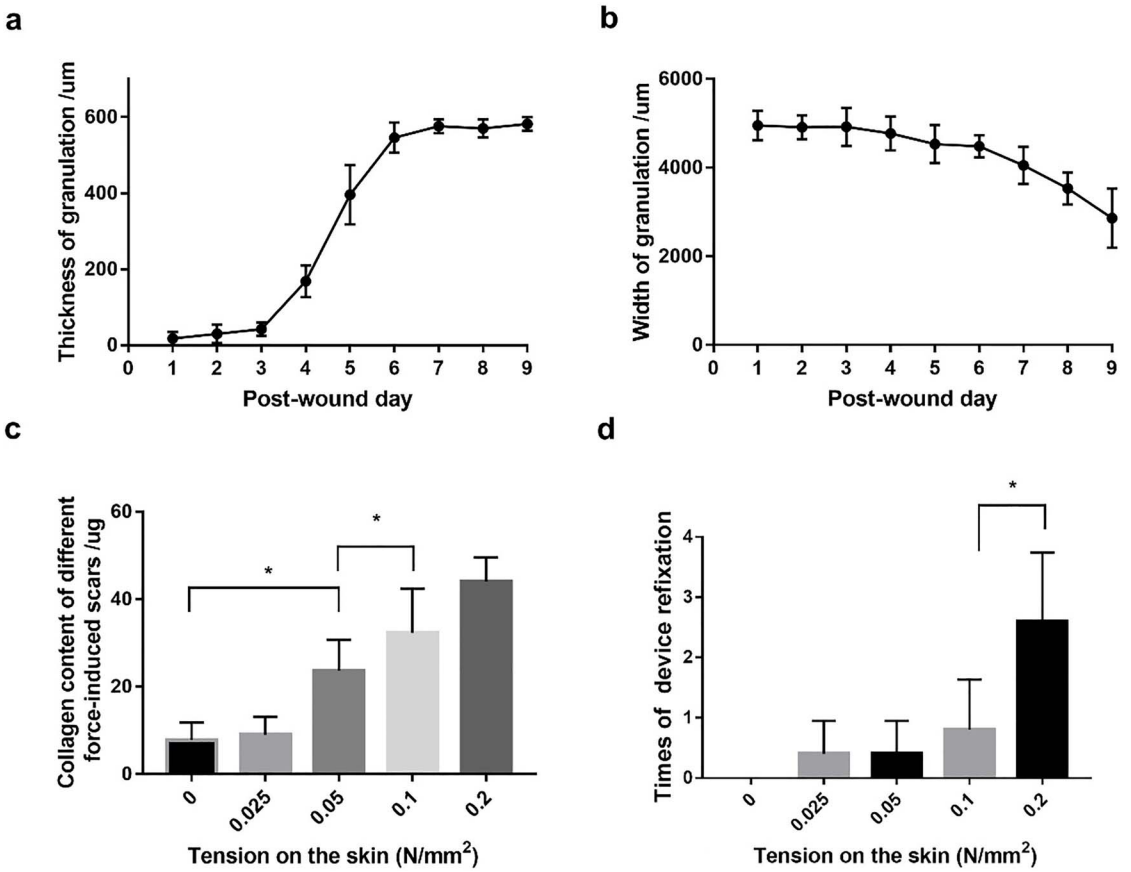

Figure 3. Time of loading and tension to induce scar. **(a)** The thickness change of the granulation after the wound was created. The granulation mostly filled the wound in 6 days. **(b)** The change of epithelial gap after the wound was created. After the first 6 days, the wound contracted dramatically. **(c)** The wound was challenged with different tension for 14 days and harvested for the measurement of collagen. **(d)** Times needed to refix the mechanical device. With 0.2 N/mm^2, times researchers needed to refix the device are significantly more

histological analysis immediately after completion of 14-day force loading and were photographed under the same condition. The surface area of each scar was measured. We found a 3.5-fold increase in scar tissue was induced by the modified method. Histologically, human hypertrophic scars include features of raised scars and a loss of rete pegs, adnexa and hair follicles. Scars induced by this modified method showed obvious and classic features of human hypertrophic scars (Fig. 5). Scar thickness and collagen density both are important characteristics of scars. The modified method increased scar thickness and produced a 2-fold greater content of collagen. However, no significant difference was found in cell density between the groups.

Discussion

Wound repair is a complex pathophysiological process composed of three consecutive and overlapping stages (15), and pathological scars are caused by an abnormal wound repair response secondary to trauma, burns and surgeries (1). During the inflammation phase, massive inflammatory cells infiltrate the wound and secrete multiple growth factors (16). During the proliferation phase, excessive deposition of extracellular matrix proteins and persistent activation of fibroblasts is apparent (17). During the remodeling phase, apoptosis is reduced. Given these abnormalities and the fact that animals are physiologically different from humans, mimicking human scars in animal models remains a major challenge for scientists and physicians.

At present, the *in vivo* model of scar can be roughly divided into three categories. The first category is to transplant a normal human skin graft (or keloid dermal graft) onto the back of a nude mouse (18). Nude mice are characterized by a deficiency in functionally mature T cells and lack of a thymus (19, 20). Although they exhibit an innate immune response and can mount a robust inflammatory response, their immunodeficiency means that they are unable to produce a normal response to specific antigens; inflammation is of great importance to scar formation. The second category is to inject profibrotic drugs subcutaneously, for example, the bleomycin-induced scar model. This model was first created by a daily injection of bleomycin subcutaneously (21). Alexander *et al.* modified this model by inserting an osmotic pump filled with bleomycin into a pocket between the skin and muscle layers to avoid daily injection (22). Many researchers have demonstrated that the epidermis plays a role

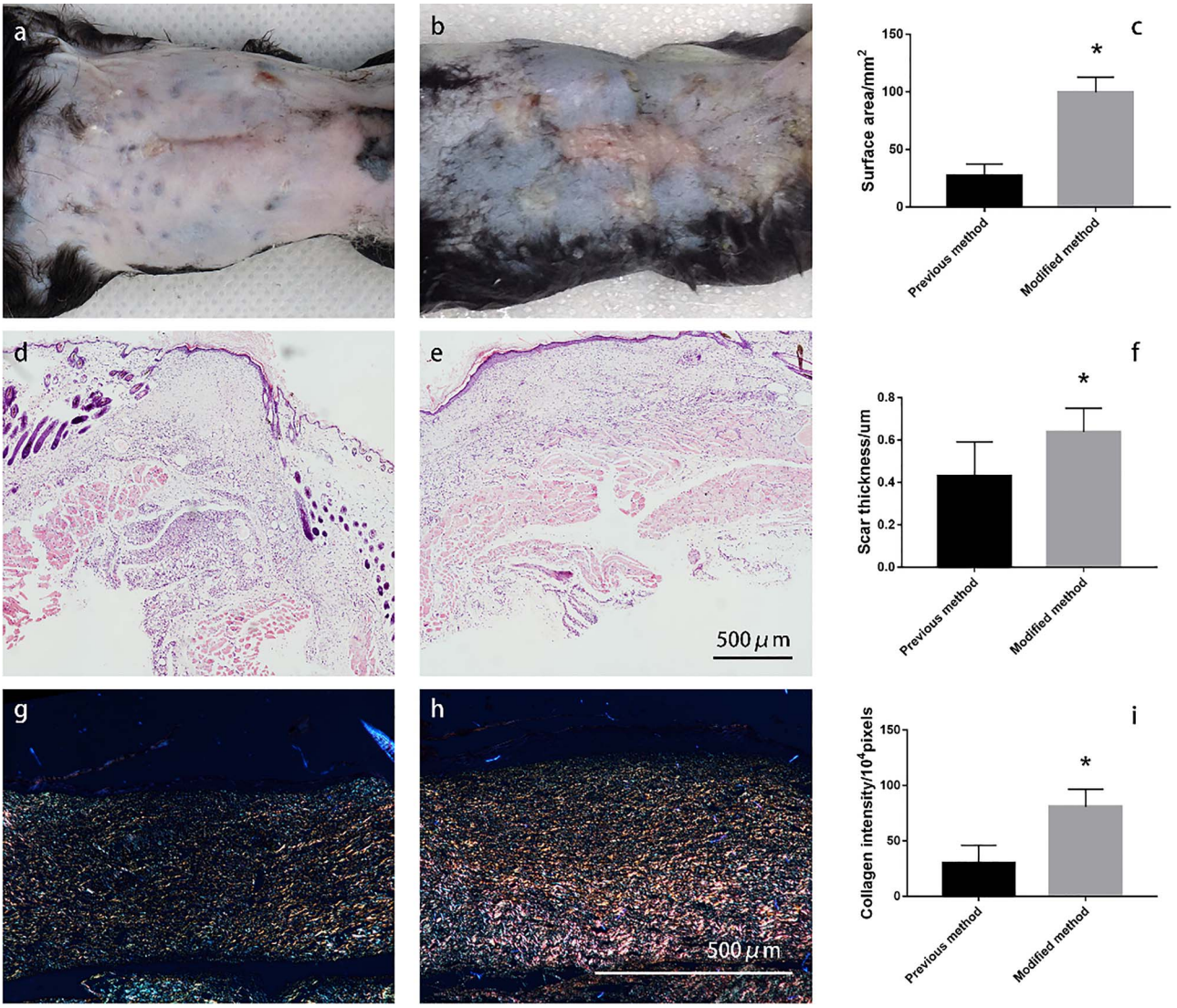

Figure 4. The modified model showed more obvious histopathological characteristics of pathological scars. The previous model is shown in the left column and the modified model is shown in the right column. **(a–c)** Mice were photographed to measure the surface area of each scar. The modified method produced significantly increased scar tissue than the previous method. (**d–f)** The histological sections were photographed and the scar thickness was measured as one of the major characteristics of pathological scars. The modified method slightly increased the thickness of the scars. **(g–i)** The sections were stained with picric acid–Sirius and photographed with microscope and polarizer accessories. The modified method produced scars with 2-fold greater collagen density. **(j–l)** Cell counting was undertaken by nuclear staining with 6-diamidino-2-phenylindole and measured with *ImageJ*. Scale bar: 500μm. There was no significant difference in cell density between the two groups

in the formation and progression of a scar (23, 24). Thus, drug injection models are restricted to studying the crosstalk between the epidermis and dermis. The final category provides additional mechanical force to reduce wound contracture and mimic scar formation. In the wound-splint model, full-thickness wounds are generated on the dorsum of the mouse, then silicone splints are fixed to the skin (13, 25). In another similar model, full-thickness and circular wounds to the depth of the surface of cartilage were generated on the ears of rabbits (26). Due to the presence of subdermal cartilage, the wounds healed clinically and were histologically similar to those of humans. However, the resting tension of skin between humans and animals is different, and these models could not provide sufficient mechanical force to completely reproduce human scars.

Aarabi *et al.* described a murine model established with mechanical force applied to a healing wound. A linear full-thickness incision on the dorsum of the mouse was made and then reapproximated with sutures. After 4 days, the sutures were removed, and the incisional scar was challenged with a stretching force provided by a skin-stretching device. Additional expansion was needed to maintain the force from the natural elongation of skin. With this model, a scar could be reproduced. Aarabi *et al.* utilized the key initiator of human scar formation, which is mechanical force, to create an ideal model. The same

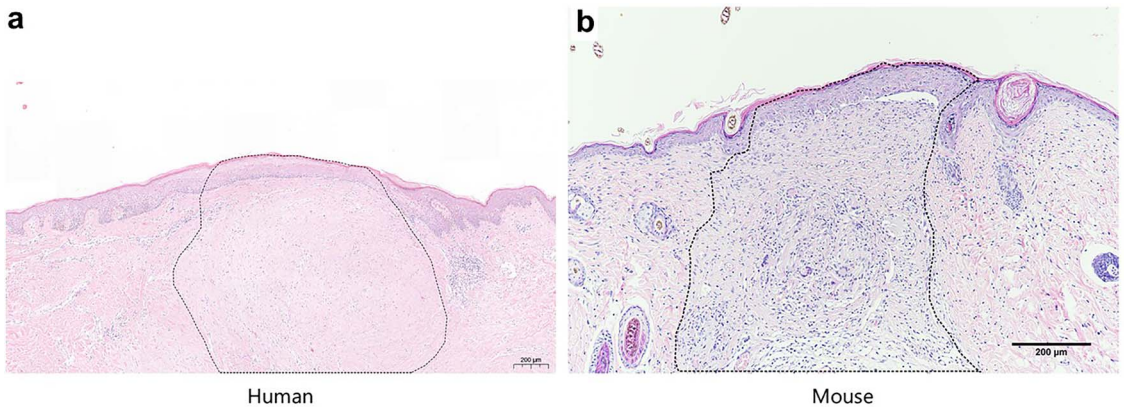

Figure 5. The modified model produced scars histologically identical to human hypertrophic scars. **(a)** Human hypertrophic scars are raised and demonstrate a loss of rete pegs, adnexa, and hair follicles. **(b)** The model mouse possesses similar classic histological features of human scars. Scale bar: 200μm

procedure could also be conducted on gene knockout mice; thus, this murine model helped researchers make a big step forward in the study of scars. However, in this model, the mechanical force applied to the wound was unmeasurable and nearly unmanageable in real-time, and tissues obtained from the wound were insufficient. Dozens of studies have used this method, but few studies have improved it.

Here, we described a modified model from Aarabi *et al.* with controlled tension on secondary wound healing in mice. Our modified procedure mainly consists of the following two parts. One was to change the healing wound from a primary closed wound to a secondary wound. We modified the linear incision to a 2×0.5 cm full-thickness wound with a silicone splint applied around the wound to avoid contracture. This procedure significantly increased the scar tissue obtained, meaning that sufficient material may be available for analysis by biomolecular techniques and flow cytometry methods. This method would also avoid the conditions of either wound dehiscence or no effect on scar formation that the previous model sometimes suffered. The other modified element of the procedure was to change the skin-stretching device from expansion screws to a device with two stainless steel plates. There were two different plates, one fixed with the screw and the other one movable. The nut was adjusted to be away from the fixed plate and compressed the spring, then the movable plate formed a controllable mechanical force on the skin. With this improvement, the mechanical force applied to the wound become measurable and controllable, making it more convenient for researchers to observe in real-time and provide timely adjustment of the tension.

It seems complicated to conduct these procedures on mice to complete this newly created model, but there are several things researchers can do to prevent models from being inaccurate. At the beginning of the experiment, mice should be fed separately to prevent the sabotage of the device, and observers need to check the devices every 12 hours and refix them if they detach from the skin.

Although the modified model generated increased scar area and increased scar thickness compared to the previous model, two weeks of observation was not enough, as murine wounds may contract without mechanical stress and the histological features may change. However, the goal of the current study was to modify the method created by Aarabi *et al.* to improve the stability and repeatability of the murine model. Therefore, the long-term results of force-induced scars were not observed.

Conclusions

The modified model we describe in this study has great potential to be applied in the study of the pathological and molecular mechanisms of scars. *In vivo* studies of new drugs and therapies designed to inhibit scar formation could also use this model. Furthermore, skin expansion (a potential application area of this model) is an important method in plastic surgery, and it is also a research focus valued by plastic surgeons. Unlike conventional expanders, this mechanical stress device would be fixed on the skin to avoid the foreign body reaction caused by the insertion of a traditional expander.

Abbreviations

SD: standard deviation

Funding

This work was supported by grants from the National Natural Science Foundation of China (81501668).

Availability of data and materials

All data generated or analysed during this study are included in this published article.

Authors' contributions

All authors were involved in the design of the study. WZ and HX were major contributors in collecting and analysing and

interpreting the data. All authors read and approved the final manuscript.

Ethics approval and consent to participate

Animal procedures were all approved by the Committee on the Ethics of Animal Experiments of Shanghai Jiao Tong University School of Medicine.

Conflicts of interest

None declared.

References

1. Sun B, Siprashvili Z, Khavari P. Advances in skin grafting and treatment of cutaneous wounds. *Science*. 2014;346:941–5.
2. Bombaro K, Engrav L, Carrougher G, Wiechman S, Faucher L, Costa B, *et al*. What is the prevalence of hypertrophic scarring following burns? *Burns*. 2003;29:299–302.
3. Wang Y, Beekman J, Hew J, Jackson S, Issler-Fisher A, Parungao R, *et al*. Burn injury: challenges and advances in burn wound healing, infection, pain and scarring. *Adv Drug Deliv Rev*. 2018;123:3–17.
4. Amini-Nik S, Yousuf Y, Jeschke M. Scar management in burn injuries using drug delivery and molecular signaling: current treatments and future directions. *Adv Drug Deliv Rev*. 2018;123:135–54.
5. Richeldi L, du Bois R, Raghu G, Azuma A, Brown K, Costabel U *et al*. Efficacy and safety of nintedanib in idiopathic pulmonary fibrosis. *N Engl J Med*. 2014;370:2071–82.
6. King T, Bradford W, Castro-Bernardini S, Fagan E, Glaspole I, Glassberg M, *et al*. A phase 3 trial of pirfenidone in patients with idiopathic pulmonary fibrosis. *N Engl J Med*. 2014;370:2083–92.
7. Marttala J, Andrews J, Rosenbloom J, Uitto J. Keloids: animal models and pathologic equivalents to study tissue fibrosis. *Matrix Biol*. 2016;51:47–54.
8. Ahn ST, Mustoe TA. Effects of ischemia on ulcer wound healing: a new model in the rabbit ear. *Ann Plast Surg*. 1990;24:17–23.
9. Falanga V, Schrayer D, Cha J, Butmarc J, Carson P, Roberts AB, *et al*. Full-thickness wounding of the mouse tail as a model for delayed wound healing: accelerated wound closure in Smad3 knock-out mice. *Wound Repair Regen*. 2004;12:320–6.
10. Reid RR, Said HK, Mogford JE, Mustoe TA. The future of wound healing: pursuing surgical models in transgenic and knockout mice. *J Am Coll Surg*. 2004;199:578–85.
11. Carlson MA, Longaker MT, Thompson JS. Wound splinting regulates granulation tissue survival. *J Surg Res*. 2003;110:304–9.
12. Davidson JM, Yu F, Opalenik SR. Splinting strategies to overcome confounding wound contraction in experimental animal models. *Adv Wound Care (New Rochelle)*. 2013;2:142–8.
13. Galiano RD, Michaels J, Dobryansky M, Levine JP, Gurtner GC. Quantitative and reproducible murine model of excisional wound healing. *Wound Repair Regen*. 2004;12:485–92.
14. Aarabi S, Bhatt K, Shi Y, Paterno J, Chang E, Loh S, *et al*. Mechanical load initiates hypertrophic scar formation through decreased cellular apoptosis. *FASEB J*. 2007;21:3250–61.
15. Singer AJ, Clark RA. Cutaneous wound healing. *N Engl J Med*. 1999;341:738–46.
16. Behm B, Babilas P, Landthaler M, Schreml S. Cytokines, chemokines and growth factors in wound healing. *J Eur Acad Dermatol Venereol*. 2012;26:812–20.
17. Bergmeier V, Etich J, Pitzler L, Frie C, Koch M, Fischer M, *et al*. Identification of a myofibroblast-specific expression signature in skin wounds. *Matrix Biol*. 2018;65:59–74.
18. Yang D, Li S, Wu J, Chen Y, Li G, Bi S, *et al*. Establishment of a hypertrophic scar model by transplanting full-thickness human skin grafts onto the backs of nude mice. *Plast Reconstr Surg*. 2007;119:104–9.
19. Festing MF, May D, Connors TA, Lovell D, Sparrow S. An athymic nude mutation in the rat. *Nature*. 1978;274:365–6.
20. Berridge MV, O'Kech N, McNeilage LJ, Heslop BF, Moore R. Rat mutant (NZNU) showing "nude" characteristics. *Transplantation*. 1979;27:410–3.
21. Yamamoto T, Takagawa S, Katayama I, Yamazaki K, Hamazaki Y, Shinkai H, *et al*. Animal model of sclerotic skin. I: local injections of bleomycin induce sclerotic skin mimicking scleroderma. *J Invest Dermatol*. 1999;112:456–62.
22. Cameron AM, Adams DH, Greenwood JE, Anderson PJ, Cowin AJ. A novel murine model of hypertrophic scarring using subcutaneous infusion of bleomycin. *Plast Reconstr Surg*. 2014;133:69–78.
23. Andriessen MP, Niessen FB, Van de Kerkhof PC, Schalkwijk J. Hypertrophic scarring is associated with epidermal abnormalities: an immunohistochemical study. *J Pathol*. 1998;186:192–200.
24. Ogawa R, Hsu CK. Mechanobiological dysregulation of the epidermis and dermis in skin disorders and in degeneration. *J Cell Mol Med*. 2013;17:817–22.
25. Jimi S, De Francesco F, Ferraro GA, Riccio M, Hara S. A novel skin splint for accurately mapping dermal Remodeling and epithelialization during wound healing. *J Cell Physiol*. 2017;232:1225–32.
26. Morris DE, Wu L, Zhao LL, Bolton L, Roth SI, Ladin DA, *et al*. Acute and chronic animal models for excessive dermal scarring: quantitative studies. *Plast Reconstr Surg*. 1997;100:674–81.